Published by
NIGERIAN SOCIETY OF PHYSICAL SCIENCES
Available online @ https://asr.nsps.org.ng/index.php/asr

African Scientific Reports 5 (2026) 438

African Scientific Reports

Perturbation and bifurcation analysis of a primary-secondary dengue infection transmission model with explicit vector dynamics and optimal control

Aloysius N. Ezaka [a,*], Henry O. Adagba [b], Sunday N. Aloke [c], Louis O. Omenyi [a], Theresa E. Efor [b], Okorie Nwite [b], Chika Agha [b]

[a] *Department of Mathematics/Statistics, Alex Ekwueme Federal University Ndufu Alike, Ebonyi State, Nigeria*
[b] *Department of Industrial Mathematics and Applied Statistics, Ebonyi State University, Abakaliki, Ebonyi State, Nigeria*
[c] *Department of Industrial Mathematics and Health Statistics, David Umahi Federal University of Health Sciences, Uburu, Ebonyi State, Nigeria*

Abstract

A robust mathematical model of multi-strain dengue infection with explicit vector dynamics is formulated to incorporate optimal control and vaccination. The bifurcation coefficients were calculated, and their numerical perturbation led to transcritical, subcritical, and supercritical bifurcations. The results showed that the effective reproduction number of the model with control is sufficiently small compared with the basic reproduction number without control. The rate of secondary infection with control, ϕ_c, was also lower than the rate of secondary infection without control, ϕ_0; that is, $\phi_c < \phi_0$. The sensitivity results showed that the mosquito-to-human and human-to-mosquito interaction rates should be targeted by control interventions to reduce infection in the population.

DOI:10.61298/asr.2026.5.2.438

Keywords: Dengue, Bifurcation, Perturbation, Reproduction number, Sensitivity

Article History:
Received: 06 January 2026
Received in revised form: 17 April 2026
Accepted for publication: 09 May 2026
Available online: 08 June 2026

1. Introduction

Dengue fever is a vector-borne infectious disease spread by the female Aedes aegypti mosquito, otherwise called yellow fever mosquito [1]. The disease has the characteristics of re-infecting an individual because of Temporal Cross-Immunity (TCI) factor in the primary infection. According to Steindorf *et al.* [2], dengue has four serotypes that co-circulate within the hosts viz: Deng-1 to Deng-4. These serotypes are associated with severe disease occasioned by the Antibody-Dependent Enhancement (ADE). The primary dengue infections are often mild [3]. However, the secondary dengue infection is characterized by a severe disease with hemorrhagic symptoms [4]. In this way persons who have experienced primary infection with one dengue type have life-long immunity against the particular type suffered. But immediately the temporary cross-immunity (TCI) time period expires, the person

*Corresponding author Tel. No.: +234-816-449-2359.
Email address: ezakaaloy@gmail.com (Aloysius N. Ezaka)

becomes prone to a distinct dengue virus type. Hence, it is only after a patient recovers from the secondary infection that such patient will have lasting immunity [5, 6].

Historically, Mathematical model explaining dengue fever infection trace back from 1970s according to Rashkov and Ko [3]. The disease is found in tropical and subtropical areas of Africa, Southeast Asia, India, China, Brazil, the Philippines, South America, Australia and South central Pacific [7]. Recently, the virus is found in three Local Government Areas of Sokoto State, Nigeria – with Sokoto South having 60 cases, Wamako having 3 cases and Dange three cases [8]. Research indicates that high rate of the disease occurrence can be witnessed in the rain forest region because of bulk vegetation cover. Both children and adults suffer dengue fever disease infection [9]. In Medpark Hospital [10], adults above 50 years and children below 15 years suffer the disease more severely. In the work by Akhil Kumar *et al.* [1], an individual can experience dengue disease more than once and are likely to develop severe dengue if experienced for the second time.

Dengue fever is a major public health threat, since over one third of the world populace are at risk of getting the disease infection [11]. Modeling estimate shows that over 380 million dengue infections occur yearly, where 96 million indicate symptoms at any stage of the disease severity. However primary natural dengue infections are often asymptomatic, but a secondary dengue infection with heterologous type constitutes the main risk factor for developing a severe dengue disease infections [1]. The Antibody-Dependent Enhancement (ADE) theory postulates that a heterotypic virus responsible for a secondary dengue infection is recognized by the antibodies produced in the first stage of the infection. This disease augmentation phenomenon and its dynamics has being used to describe the etiology of severe disease indicated to have correlated with higher viral load [2].

Aedes aegypti spread different viruses to humans, such as yellow fever virus, chikungunya virus, Zika virus and dengue virus, a phenomenon called arboviruses [10]. The spread of the disease is via mosquito bite and sucking blood meal of the human hosts, while non-vector transmission of the disease occurs through blood transfusion, bone-marrow transplanting and breast feeding [12]. Mosquitoes get the dengue virus immediately they take blood meal from the persons having the virus in their blood stream [1]. However, dengue symptoms include mild fever to incapacitating high fever alongside with severe headache, rashes, muscle and joint pains, dengue shock syndrome, respiratory distress, severe bleeding and serious organ impairment [9]. The Centers for Disease Control and Prevention [9] made it known that Dengue has three identified clinical phases that can be incorporated into this model viz: the febrile phase characterized by feverish signs. The second phase is the critical phase. It is the period of potential plasma leakage that cause dehydration, reduced urination and organ malfunction. The third phase is the period of convalescent. It is the recovery period when re-absorption begins while plasma leakage stops. Dengue fever infection is noticed after the incubation period of 4 to 10 days in humans, after the bite of mosquito. The incubation period of the virus is 8 to 12 days within the mosquito [10].

However, prevention involves mosquito control measures and avoiding mosquito bites by using mosquito treated nets and good environmental sanitation as stipulated by the Centers for Disease Control and Prevention [9]. However, because of the complex nature of dengue disease, vaccines have been developed to provide long term protection against every dengue virus serotypes [13]. These vaccines are safe, effective and affordable geared towards the control of the disease. The vaccines are crucial for reducing dengue spread and mortality. According to research findings by Steindorf *et al.* [2], two tetravalent dengue vaccines have been discovered; the Dengvaxia produced by Sanofi Pasteur that is now licensed in more than 20 Countries. The second one is QDeng or Dengvax vaccine produced by Takeda Pharmaceutical company. The two vaccines, according to Mayo Clinic [14] are to be administered at secondary infection level where the severity of the infection is high. While Aguiar *et al.* [15] in their research made it known that in the absence of an effective and safe dengue vaccines, vector control remains the only alternative to preventing dengue transmission.

2. Materials and methods

We formulate a modified SIR-SIR model by extending an existing one to incorporate optimal vector control and preventive vaccination. We let N and M be the Total human and Mosquito populations respectively, S be the Susceptible humans with no history of Dengue infection, I_p be the Primary Infected individuals, R_p be Recovered individuals from primary infection with temporary immunity, S_p be Susceptible persons with history of Dengue infection, I_s be the Secondary infected individuals due to disease enhancement factor, R be the Recovered individuals from secondary infection with long-term immunity, S_v be Susceptible Mosquitoes, I_v be the Infected Mosquitoes, Λ be the Recruitments into the human population, Ω be the Recruitment into the mosquito population, δ be the Use of mosquito treated nets, θ be the good environmental sanitation, τ be Effective Vaccine, β be Transmission rate or interaction rate from vector to humans, ϑ be Transmission rate or interaction rate from humans to vector, γ be Recovery rate of humans, α be the Temporary immunity rate crossed to secondary infections, ϕ be the Rate of secondary infection to overall force of infection, μ be the Natural mortality rate of humans, ν be the Natural mortality rate of mosquitoes.

2.1. Assumptions of the model

1. Recruitment into the human population are both children and Adults,
2. Natural mortality and birth rates are not equal in both human and vector populations,
3. Individuals die due to the disease at the rate η and σ and naturally at the rate μ,
4. Mosquitoes die due to the disease at the rate ω and naturally at the rate ν,

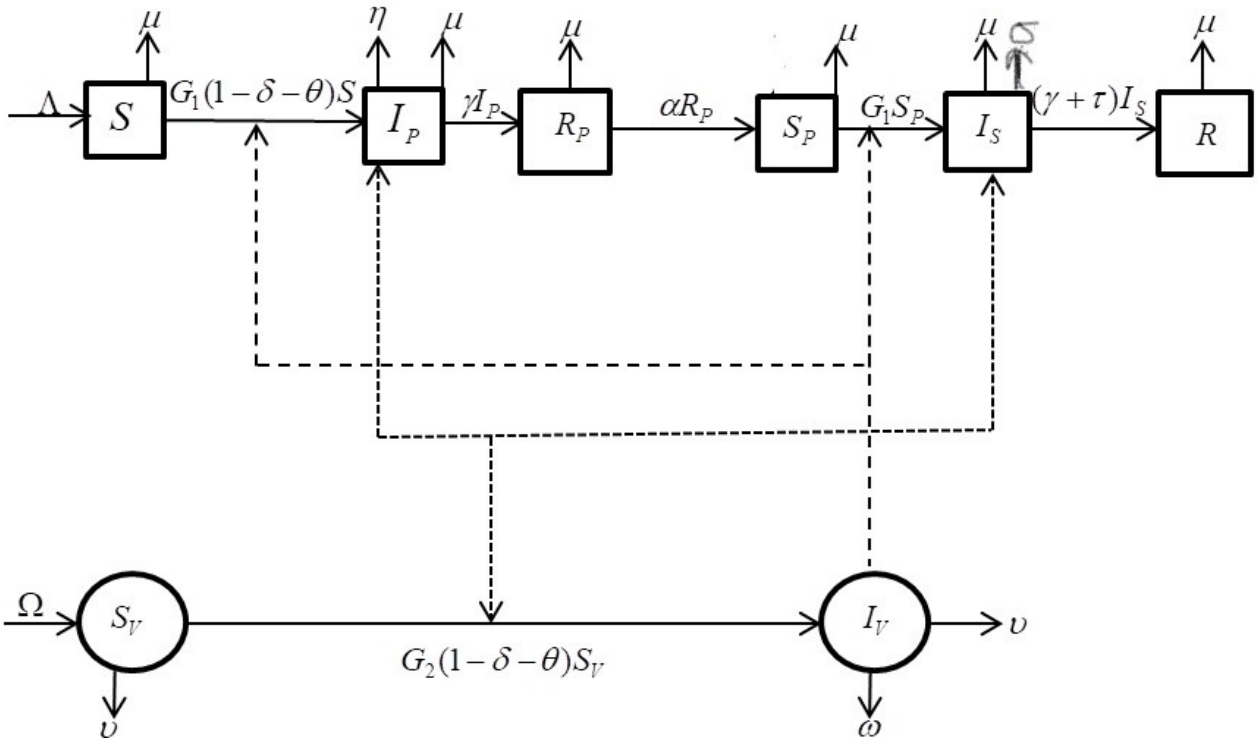

Figure 1. The extended schematic diagram of Dengue.

5. Recovery is by clinical treatment,
6. Individuals recover from primary infection with temporal immunity,
7. Severe disease occurs at secondary infection due to ADE process,
8. Vector controls are by the use of mosquito treated nets and good environmental sanitation while prevention is by vaccination,
9. Individuals in secondary infection transmit more of the disease if $\phi > 1$ and less if ϕ is less than one.

However, the total population as function of t for both humans and mosquitoes are $N(t) = S(t) + I_p(t) + R_p(t) + S_p(t) + I_s(t) + R(t)$ and $M(t) = S_v(t) + I_v(t)$ respectively. The Extended Model Equations are as follows:

$$\left.\begin{array}{rcl} \frac{dS}{dt} &=& \Lambda - G_1(1-\delta-\theta)S - \mu S, \\ \frac{dI_p}{dt} &=& G_1(1-\delta-\theta)S - (\mu+\gamma+\eta)I_p, \\ \frac{dR_p}{dt} &=& \gamma I_p - (\mu+\alpha)R_p, \\ \frac{dS_p}{dt} &=& \alpha R_p - G_1 S_p - \mu S_p, \\ \frac{dI_s}{dt} &=& G_1 S_p - (\gamma+\tau)I_s - \mu I_s - \sigma I_s, \\ \frac{dR}{dt} &=& (\gamma+\tau)I_s - \mu R, \\ \frac{dS_v}{dt} &=& \Omega - G_2(1-\delta-\theta)S_v - \nu S_v, \\ \frac{dI_v}{dt} &=& G_2(1-\delta-\theta)S_v - (\nu+\omega)I_v, \end{array}\right\} \quad (1)$$

where

$$G_1 = \frac{\beta}{M} I_v,$$

and

$$G_2 = \frac{\vartheta}{N} I_p + \frac{\vartheta}{N}\phi I_s.$$

The extended schematic diagram is represented in Figure 1.

2.2. Positivity of solutions

The positivity in this model indicates a fundamental constraint which ensures that all state variables remain greater than or equal to zero for all time $t \geq 0$. It is a critical requirement for a model to be physically meaningful.

Theorem 1. *Let the initial data* $(S(0), I_p(0), R_p(0), S_p(0), I_s(0), R(0), S_v(0), I_v(0)) \geq 0 \in R_+^8$. *Then, the solution set* $(S(t), I_p(t), R_p(t), S_p(t), I_s(t), R(t), S_v(t), I_v(t))$ *of the model are positive for all* $t \geq 0$.

Proof. From the model equation (1)

$$\begin{aligned}
\frac{dS}{dt} &= \Lambda - G_1(1-\delta-\theta)S - \mu S, \\
&\geq -(G_1(1-\delta-\theta)+\mu)S, \\
\int \frac{1}{S} dS &\geq -(G_1(1-\delta-\theta)+\mu)\int dt, \\
\ln S &\geq -(G_1(1-\delta-\theta)+\mu)t + c, \\
S &\geq A_1 e^{-(G_1(1-\delta-\theta)+\mu)t}.
\end{aligned}$$

Hence the solution with initial condition becomes $S(t) \geq S(0)e^{-(G_1(1-\delta-\theta)+\mu)t} > 0$, which implies that $S(t) > 0$. Applying similar method to other state variables, we have that $I_p(t) \geq 0$, $R_p(t) \geq 0$, $S_p(t) \geq 0$, $I_s(t) \geq 0$, $R(t) \geq 0$, $S_v(t) > 0$, and $I_v(t) \geq 0$. ■

2.3. Boundedness of solutions

In this section, we show that the model system of equations have differentiable properties and bounded above by $\frac{\Lambda}{\mu}$.

Theorem 2. *Let* $D \subset R_+^6$ *be the set, then the solution set* $X(t) = (S + I_p + R_p + S_p + I_s + R) \in D \subset R_+^6$ *of model equation (1) are feasible for all* $t \geq 0$.

Proof. We require to prove that the solution set X(t) are attainable in the Domain $D \subset R_+^6$. Let $X(t) = (S + I_p + R_p + S_p + I_s + R) \in D \subset R_+^6$ be the solution of the system with positive initial condition.

The total population of human host is given by: $N = S + I_p + R_p + S_p + I_s + R$.

$$\begin{aligned}
\frac{dN}{dt} &= \frac{dS}{dt} + \frac{dI_p}{dt} + \frac{dR_p}{dt} + \frac{dS_p}{dt} + \frac{dI_s}{dt} + \frac{dR}{dt} \\
&= \Lambda - \mu(S + I_p + R_p + S_p + I_s + R) - \eta I_p - \sigma I_s \\
&= \Lambda - \mu N - \eta I_p - \sigma I_s.
\end{aligned}$$

That of vector population is given by: $M = S_v + I_v$,

$$\frac{dM}{dt} = \frac{dS_v}{dt} + \frac{dI_v}{dt} = \Omega - \nu M.$$

In the absence of the disease infection, the human population is resolved as follows:

$$\frac{dN}{dt} = \Lambda - \mu N - \eta I_p - \sigma I_s \leq \Lambda - \mu N,$$

$$\frac{dN}{dt} \leq \Lambda - \mu N.$$

By separation of variables,

$$\ln(\Lambda - \mu N) \geq -\mu(t + c),$$

then

$$N(t) \leq \frac{\Lambda - Ae^{-\mu t}}{\mu}.$$

Applying the initial condition $N(0) = N0$, the solution becomes

$$N(t) \leq \frac{\Lambda - N(0)e^{-\mu t}}{\mu} \text{ as } t \to \infty.$$

Hence,

$$0 < N(t) \leq \frac{\Lambda}{\mu}.$$

Similarly, that of mosquito population gives

$$0 < M(t) \leq \frac{\Omega}{\nu}.$$

Therefore, the population is analytic since the upper bound limit $\frac{\Lambda}{\mu}$ and $\frac{\Omega}{\nu}$exists. ■

2.4. Existence of disease-free and endemic equilibria

The extended model admits disease-free and endemic equilibria.

$$\frac{dS}{dt} = 0 \Rightarrow \Lambda - \left(\frac{\beta}{M}(1-\delta-\theta)I_V + \mu\right)S = 0,$$
$$\Lambda = \left(\frac{\beta}{M}(1-\delta-\theta)I_V + \mu\right)S.$$

In the absence of the infection, $I_V = 0$, hence $S = \frac{\Lambda}{\mu}$. Similarly, $I_p = 0, R_p = 0$, $S_p = 0$, $I_s = 0$, $R = 0$, $S_v = \frac{\Omega}{\nu}$ and $I_v = 0$.
On the other hand, in the presence of the dengue infection then $I_p \neq 0, R_p \neq 0$, $S_p \neq 0$, $I_s \neq 0$, $R \neq 0$, $S \neq 0$, $S_v \neq 0$, $I_v \neq 0, N \neq 0$, $M \neq 0$. Hence, the steady state of the model at Endemic Equilibrium (EE) state is given by $(x_*) = (S^*, I_p^*, R_p^*, S_p^*, I_s^*, R^*, I_v^*, S_v^*)$,

$$S^* = \frac{\Lambda}{\mu + G_1(1-\delta-\theta)},$$
$$I_p^* = \frac{\Lambda G_1(1-\delta-\theta)}{(\mu+\gamma+\eta)(\mu+G_1(1-\delta-\theta))},$$
$$R_p^* = \frac{\gamma\Lambda G_1(1-\delta-\theta)}{(\mu+\alpha)(\mu+\gamma+\eta)(\mu+G_1(1-\delta-\theta))},$$
$$S_p^* = \frac{\alpha\gamma\Lambda}{(G_1+\mu)(\mu+\alpha)(\mu+\gamma+\eta)(\mu+G_1(1-\delta-\theta))},$$
$$I_s^* = \frac{G_1\alpha\gamma\Lambda}{(\mu+\gamma+\tau+\sigma)(G_1+\mu)(\mu+\alpha)(\mu+\gamma+\eta)(\mu+G_1(1-\delta-\theta))},$$
$$R^* = \frac{G_1\alpha\gamma\Lambda(\gamma+\tau)}{\mu(\mu+\gamma+\tau+\sigma)(G_1+\mu)(\mu+\alpha)(\mu+\gamma+\eta)(\mu+G_1(1-\delta-\theta))},$$
$$S_v^* = \frac{\Omega}{G_2(1-\delta-\theta)+\nu},$$
$$I_v^* = \frac{\Omega G_2(1-\delta-\theta)}{(\nu+\omega)(G_2(1-\delta-\theta)+\nu)}.$$

2.5. Perturbation analysis of the model

Lemma: The equilibrium solutions of the model exhibit subcritical and supercritical bifurcations [16, 17]. proof
We now use perturbation technique to assess the considerable deviation from the original or unperturbed problem to a new or perturbed system. Perturbation results in different behaviours of the model and hence different portraits [18]. The difference between the perturbed and unperturbed solutions gives the asymptotic approximation of the model solution [19]. We introduce a small parameter $\epsilon \ll 1$ representing the magnitude of infection and expand all variables as:

$$X(t) = X^{(0)}(t) + \epsilon X^{(1)}(t) + O(\epsilon^2), \tag{2}$$

for each state variable, with the infectious classes being of order ϵ:

$$I_p = \epsilon I_p^{(1)} + O(\epsilon^2), \quad I_s = \epsilon I_s^{(1)} + O(\epsilon^2), \quad I_v = \epsilon I_v^{(1)} + O(\epsilon^2). \tag{3}$$

Zeroth-order solution (ϵ^0)

At zeroth order, setting $\epsilon = 0$ (i.e., $I_p = I_s = I_v = 0$), we have $G_1^{(0)} = 0$ and $G_2^{(0)} = 0$. The system reduces to:

$$\frac{dS^{(0)}}{dt} = \Lambda - \mu S^{(0)},$$
$$\frac{dI_p^{(0)}}{dt} = 0 \Rightarrow I_p^{(0)} = 0,$$
$$\frac{dR_p^{(0)}}{dt} = -(\mu+\alpha)R_p^{(0)} \Rightarrow R_p^{(0)} = 0,$$
$$\frac{dS_p^{(0)}}{dt} = -\mu S_p^{(0)} \Rightarrow S_p^{(0)} = 0,$$

$$\frac{dI_s^{(0)}}{dt} = -(\gamma + \tau + \mu + \sigma)I_s^{(0)} \Rightarrow I_s^{(0)} = 0,$$
$$\frac{dR^{(0)}}{dt} = -\mu R^{(0)} \Rightarrow R^{(0)} = 0,$$
$$\frac{dS_v^{(0)}}{dt} = \Omega - \nu S_v^{(0)},$$
$$\frac{dI_v^{(0)}}{dt} = 0 \Rightarrow I_v^{(0)} = 0.$$

Solving these:

$$S^{(0)}(t) = S(0)e^{-\mu t} + \frac{\Lambda}{\mu}(1 - e^{-\mu t}), \tag{4}$$
$$S_v^{(0)}(t) = S_v(0)e^{-\nu t} + \frac{\Omega}{\nu}(1 - e^{-\nu t}), \tag{5}$$

with all infected and recovered classes identically zero:

$$I_p^{(0)}(t) = R_p^{(0)}(t) = S_p^{(0)}(t) = I_s^{(0)}(t) = R^{(0)}(t) = I_v^{(0)}(t) = 0. \tag{6}$$

At steady state ($t \to \infty$), the disease-free equilibrium (DFE) is:

$$S^{(0)*} = \frac{\Lambda}{\mu}, \quad S_v^{(0)*} = \frac{\Omega}{\nu}, \quad \text{others } 0. \tag{7}$$

At this equilibrium, $N^{(0)} = S^{(0)*} = \frac{\Lambda}{\mu}$ and $M^{(0)} = S_v^{(0)*} = \frac{\Omega}{\nu}$.

First-order equations (ϵ^1)

First, we compute the first-order terms of the infection rates. Expanding:

$$G_1 = \frac{\beta}{M} I_v = \frac{\beta}{M^{(0)} + \epsilon M^{(1)} + \cdots} \cdot \epsilon I_v^{(1)} + \cdots = \epsilon \frac{\beta}{M^{(0)}} I_v^{(1)} + O(\epsilon^2), \tag{8}$$
$$G_2 = \frac{\vartheta}{N} I_p + \frac{\vartheta}{N} \phi I_s = \frac{\vartheta}{N^{(0)} + \epsilon N^{(1)} + \cdots} \left(\epsilon I_p^{(1)} + \epsilon \phi I_s^{(1)}\right) + \cdots, \tag{9}$$
$$= \epsilon \frac{\vartheta}{N^{(0)}} \left(I_p^{(1)} + \phi I_s^{(1)}\right) + O(\epsilon^2). \tag{10}$$

Thus,

$$G_1^{(1)} = \frac{\beta}{M^{(0)}} I_v^{(1)}, \quad G_2^{(1)} = \frac{\vartheta}{N^{(0)}} \left(I_p^{(1)} + \phi I_s^{(1)}\right). \tag{11}$$

Collecting terms of order ϵ from each equation, the first order is given as: The first-order equations form a linear system:

$$\frac{dS^{(1)}}{dt} = -\frac{\beta}{M^{(0)}} I_v^{(1)} S^{(0)} - \mu S^{(1)},$$
$$\frac{dI_p^{(1)}}{dt} = \frac{\beta}{M^{(0)}} I_v^{(1)} S^{(0)} - (\mu + \gamma + \eta) I_p^{(1)},$$
$$\frac{dR_p^{(1)}}{dt} = \gamma I_p^{(1)} - (\mu + \alpha) R_p^{(1)},$$
$$\frac{dS_p^{(1)}}{dt} = \alpha R_p^{(1)} - \mu S_p^{(1)},$$
$$\frac{dI_s^{(1)}}{dt} = \frac{\beta}{M^{(0)}} I_v^{(1)} S_p^{(1)} - (\gamma + \tau + \mu + \sigma) I_s^{(1)},$$
$$\frac{dR^{(1)}}{dt} = (\gamma + \tau) I_s^{(1)} - \mu R^{(1)},$$
$$\frac{dS_v^{(1)}}{dt} = -\frac{\vartheta}{N^{(0)}} \left(I_p^{(1)} + \phi I_s^{(1)}\right) S_v^{(0)} - \nu S_v^{(1)},$$
$$\frac{dI_v^{(1)}}{dt} = \frac{\vartheta}{N^{(0)}} \left(I_p^{(1)} + \phi I_s^{(1)}\right) S_v^{(0)} - (\nu + \omega) I_v^{(1)}.$$

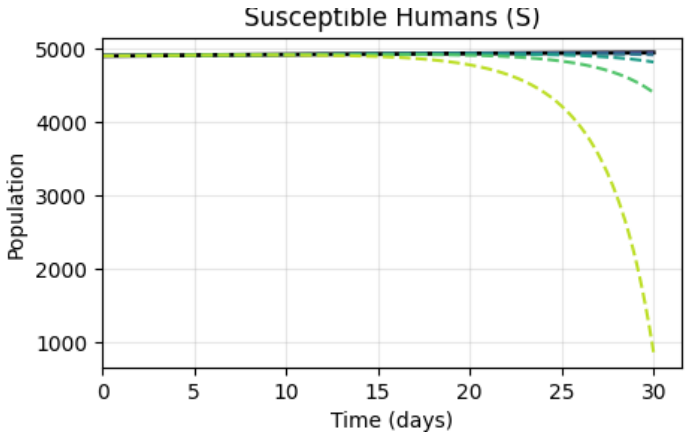

Figure 2. Perturbation result for S class.

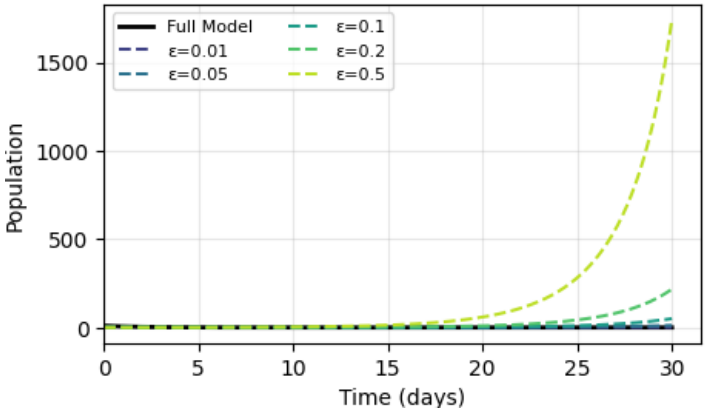

Figure 3. Perturbation result for I_P class.

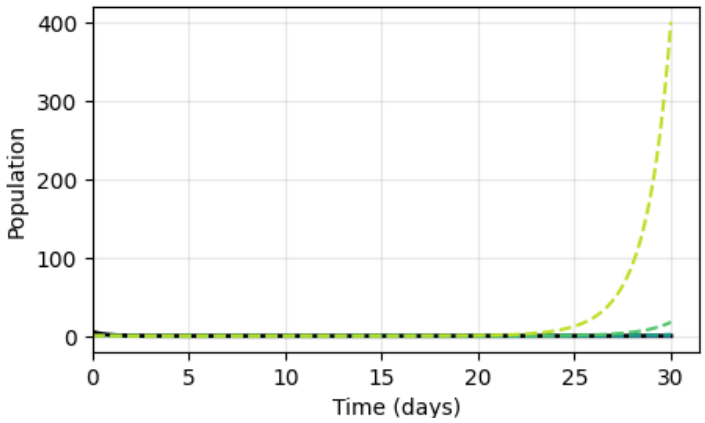

Figure 4. Perturbation result for I_S class.

The graphs show the graphical representation of the perturbation analysis:

This compartment represents the susceptible population. The population is constant in the absence of the disease but when the system is perturbed, the population begins to decline. This compartment represents the population of infected individuals at the primary state. The population is zero in the absence of the disease and the population increases when the system is perturbed. This compartment represents the population of infected individuals at the secondary state as a result of being reinfected after recovery from the primary stage. The population is zero in the absence of the disease and the population increases when the system is perturbed. This compartment represents the population of infected mosquito. In the absence of the disease, the population is zero and the population increases when the system is perturbed.

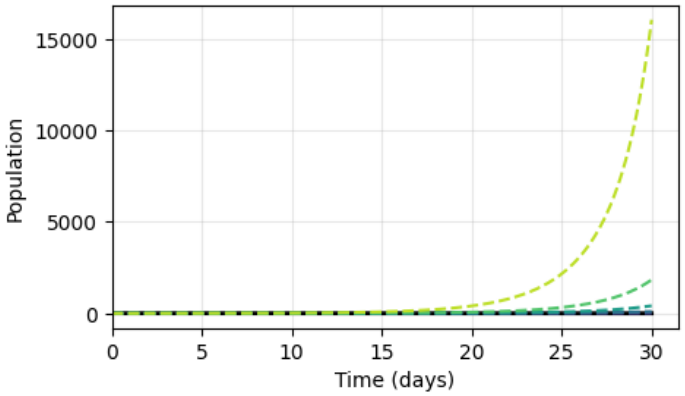

Figure 5. Perturbation result for the infected mosquito class.

2.6. Computation of the effective and basic reproduction numbers

In this section we use the next generation matrix in Ref. [20]. The Model is decomposed into two transition matrices F and V representing the inflow and outflow of the system as follows:

$$x_j' = f_i(x) - v_i(x),$$

$$F = \left(\frac{\partial f_i}{\partial x_j}\right)\Big|_{x^0}, \quad V = \left(\frac{\partial v_i}{\partial x_j}\right)\Big|_{x^0},$$

where F and V are $m \times m$ matrices of partial derivatives of the transition matrices f_i and v_i respectively, and represent the infectious compartments.
$x_j = I_p\ , I_s\ , I_v$ and $x_j' = \partial I_p\ , \partial I_s\ , \partial I_v$. where $1 \le i, j \le m$.

$$f_i = \begin{pmatrix} \frac{\beta}{M} I_v(1-\delta-\theta)S \\ \frac{\beta}{M} I_v S_p \\ \frac{\vartheta}{N} S_v(I_p + \phi I_s) \end{pmatrix}, \quad v_i = \begin{pmatrix} (\mu+\gamma+\eta)I_p \\ (\gamma+\tau+\mu+\sigma)I_s \\ (\nu+\omega)I_v \end{pmatrix}$$

$$F = \begin{pmatrix} 0 & 0 & \frac{\beta}{M} S(1-\delta-\theta) \\ 0 & 0 & 0 \\ \frac{\vartheta}{N} S_v & \frac{\vartheta}{N}\phi S_v & 0 \end{pmatrix}, \quad V = \begin{pmatrix} (\mu+\gamma+\eta) & 0 & 0 \\ 0 & (\gamma+\tau+\mu+\sigma) & 0 \\ 0 & 0 & (\nu+\omega) \end{pmatrix},$$

$$V^{-1} = \begin{pmatrix} \frac{1}{\mu+\gamma+\eta} & 0 & 0 \\ 0 & \frac{1}{\gamma+\tau+\mu+\sigma} & 0 \\ 0 & 0 & \frac{1}{\nu+\omega} \end{pmatrix} \text{ then } FV^{-1} = \begin{pmatrix} 0 & 0 & \frac{\beta S(1-\delta-\theta)}{M(\nu+\omega)} \\ 0 & 0 & 0 \\ \frac{\vartheta S_v}{N(\mu+\gamma+\eta)} & \frac{\vartheta\phi S_v}{N(\gamma+\tau+\mu+\sigma)} & 0 \end{pmatrix}.$$

The basic reproduction number R_0 is the spectral radius of FV^{-1}:

$$R_0 = \sqrt{\frac{\beta\vartheta}{(\mu+\gamma+\eta)(\nu+\omega)}} = 2.309114 > 1.$$

The effective reproduction number with control is:

$$R_e = \sqrt{\frac{\beta\vartheta(1-\delta-\theta)}{(\mu+\gamma+\eta)(\nu+\omega)}} = 0.326557996 < 1.$$

It is observed that $R_e < R_0$ whenever controls are effective.

2.7. Analysis of the disease-free equilibrium

Next, we use the classical linearization Theorem- The Routh-Hurwitz Criterion to assess the local stability of the model.

Theorem 3. *Given a coefficient Matrix (M), the Equilibrium point is called Asymptotically stable if:* $Tr(J(M))_{DFE} < 0$ *and* $Det(J(M))_{DFE} > 0$ *[21].*

Table 1. Parameter values used in the model.

Parameters	Description	values	Source
Λ	Recruitment into susceptible population	100	[1]
Ω	Recruitment into vector population	1000	[1]
δ	Use of ITNs	0.44	Assumed
θ	Good environmental sanitation	0.54	Assumed
τ	vaccination	0.95	[15]
β	Transmission rate from vector to human	0.5	[1]
ϑ	Transmission rate from human to vectors	0.75	[15]
γ	Recovery rate of human	0.52	[1]
α	Temporal immunity rate	0.5	[1]
ϕ	Rate of secondary infection to overall force of infection	2.6	[1]
μ	Natural mortality rate for humans	0.02	[1]
ν	Natural mortality for mosquito	0.03	[1]
ω	Induced death rate	0.1	[15]
η	Induced death rate of I_P class	0.001	[15]
σ	Induced death rate for I_S	0.002	Assumed

Proof. We set the equations of the model as

$$\left.\begin{array}{rcl} f_1 &=& \Lambda - G_1(1-\delta-\theta)S - \mu S, \\ f_2 &=& G_1(1-\delta-\theta)S - (\mu+\gamma+\eta)I_p, \\ f_3 &=& \gamma I_p - (\mu+\alpha)R_p, \\ f_4 &=& \alpha R_p - G_1 S_p - \mu S_p, \\ f_5 &=& G_1 S_p - (\gamma+\tau)I_s - \mu I_s - \sigma I_s, \\ f_6 &=& (\gamma+\tau)I_s - \mu R, \\ f_7 &=& \Omega - G_2(1-\delta-\theta)S_v - \nu S_v, \\ f_8 &=& G_2(1-\delta-\theta)S_v - (\nu+\omega)I_v. \end{array}\right\} \tag{12}$$

The Jacobian Matrix is given below

$$J = \begin{pmatrix} -\mu & 0 & 0 & 0 & 0 & 0 & 0 & -\frac{\beta\Lambda(1-\delta-\theta)}{M\mu} \\ 0 & -(\mu+\gamma+\eta) & 0 & 0 & 0 & 0 & 0 & \frac{\beta\Lambda(1-\delta-\theta)}{M\mu} \\ 0 & \gamma & -(\mu+\alpha) & 0 & 0 & 0 & 0 & 0 \\ 0 & 0 & \alpha & -\mu & 0 & 0 & 0 & 0 \\ 0 & 0 & 0 & 0 & -(\gamma+\tau+\mu+\sigma) & 0 & 0 & 0 \\ 0 & 0 & 0 & 0 & (\gamma+\tau) & -\mu & 0 & 0 \\ 0 & -\frac{\vartheta\Omega(1-\delta-\theta)}{N\nu} & 0 & 0 & -\frac{\vartheta\phi\Omega(1-\delta-\theta)}{N\nu} & 0 & -\nu & 0 \\ 0 & \frac{\vartheta\Omega(1-\delta-\theta)}{N\nu} & 0 & 0 & \frac{\vartheta\phi\Omega(1-\delta-\theta)}{N\nu} & 0 & 0 & -(\nu+\omega) \end{pmatrix}.$$

The trace of the above Jacobian matrix is given as: $Tr(J) = -5\mu - 2\gamma - \eta - \tau - \sigma - 2\nu - \omega$ and substituting the parameters values, we have $Tr(J) = -2.253 < 0$. The characteristic equation is given by:

$$\det(J-\lambda I) = \begin{vmatrix} -\mu-\lambda & 0 & 0 & 0 & 0 & 0 & 0 & -\frac{\beta\Lambda(1-\delta-\theta)}{M\mu} \\ 0 & -m-\lambda & 0 & 0 & 0 & 0 & 0 & \frac{\beta\Lambda(1-\delta-\theta)}{M\mu} \\ 0 & \gamma & -(\mu+\alpha)-\lambda & 0 & 0 & 0 & 0 & 0 \\ 0 & 0 & \alpha & -\mu-\lambda & 0 & 0 & 0 & 0 \\ 0 & 0 & 0 & 0 & -q-\lambda & 0 & 0 & 0 \\ 0 & 0 & 0 & 0 & (\gamma+\tau) & -\mu-\lambda & 0 & 0 \\ 0 & -\frac{\vartheta\Omega(1-\delta-\theta)}{N\nu} & 0 & 0 & -\frac{\vartheta\phi\Omega(1-\delta-\theta)}{N\nu} & 0 & -\nu-\lambda & 0 \\ 0 & \frac{\vartheta\Omega(1-\delta-\theta)}{N\nu} & 0 & 0 & \frac{\vartheta\phi\Omega(1-\delta-\theta)}{N\nu} & 0 & 0 & -(\nu+\omega)-\lambda \end{vmatrix} = 0,$$

where $m = \mu+\gamma+\eta$ and $q = \gamma+\tau+\mu+\sigma$. The eigenvalues are: $\lambda_1 = -\mu < 0$, $\lambda_2 = -(\mu+\alpha) < 0$, $\lambda_3 = -\mu < 0$, $\lambda_4 = -(\gamma+\tau+\mu+\sigma) < 0$, $\lambda_5 = -\mu < 0$, $\lambda_6 = -\nu < 0$ while the two other eigenvalues are determined as the roots of the quadratic equation $a_1\lambda^2 + a_2\lambda + a_3 = 0$, where $a_1 = 1 > 0, a_2 = (\nu+\omega+\gamma+\tau+\mu+\sigma) > 0$ and $a_3 = (\nu+\omega)(\gamma+\tau+\mu+\sigma)(1-R_e) > 0$, for $R_e < 1$. According to Routh-Hurwtiz Criterion, $a_1 > 0$, $a_1a_2 - a_3 > 0$ ensures that the DFE is asymptotically stable whenever $R_e < 1$. ■

2.8. Stability analysis using bifurcation

At bifurcation, $R_e = 1$. Reproduction number of infection is essential in this section because it represents the spreading of infection [1, 21]. Recall that

$$R_e = \sqrt{\frac{\beta\vartheta(1-\delta-\theta)}{(\mu+\gamma+\eta)(\nu+\omega)}} \leq \frac{\beta\vartheta(1-\delta-\theta)}{(\mu+\gamma+\eta)(\nu+\omega)}.$$

Let $\psi = \beta$ be the bifurcation parameter and $R_e = 1$ be the bifurcation point. Then

$$R_e = 1 = \frac{\Psi\vartheta(1-\delta-\theta)}{(\mu+\gamma+\eta)(\nu+\omega)}.$$

$$\psi = \frac{(\mu+\gamma+\eta)(\nu+\omega)\mu\nu}{\vartheta(1-\delta-\theta)}.$$

From the foregoing, R_e is directly proportional to the bifurcation parameter Ψ, because increase in the value of the bifurcation parameter will bring a considerable increase in the effective reproduction number R_e of the Dengue infectious disease and vice versa [18]. Now, the differential equations of the model are expressed as

$$\frac{dx}{dt} = f(x, \Psi),$$

where x is an 8-dimensional vector with compartments

$$x = (x_1, x_2, x_3, x_4, x_5, x_6, x_7, x_8)^T,$$

corresponding to the State variables $(S, I_p, R_p, S_p, I_s, R, S_v, I_v)$ respectively. Hence the function

$$f : R^8 \times R \to R^8.$$

$$f = (f_1, f_2, f_3, f_4, f_5, f_6, f_7, f_8).$$

Hence, the model equations can be re-written as

$$\left.\begin{array}{rcl} f_1 &=& \Lambda - \frac{\Psi}{M}(1-\delta-\theta)x_1x_8 - \mu x_1, \\ f_2 &=& \frac{\Psi}{M}(1-\delta-\theta)x_1x_8 - (\mu+\gamma+\eta)x_2, \\ f_3 &=& \gamma x_2 - (\mu+\alpha)x_3, \\ f_4 &=& \alpha x_3 - \frac{\Psi}{M}x_4x_8 - \mu x_4, \\ f_5 &=& \frac{\Psi}{M}x_4x_8 - (\gamma+\tau)x_5 - \mu x_5 - \sigma x_5, \\ f_6 &=& (\gamma+\tau)x_5 - \mu x_6, \\ f_7 &=& \Omega - \left(\frac{\vartheta}{N}x_2 + \frac{\phi\vartheta}{N}x_5\right)(1-\delta-\theta)x_7 - \nu x_7, \\ f_8 &=& \left(\frac{\vartheta}{N}x_2 + \frac{\phi\vartheta}{N}x_5\right)(1-\delta-\theta)x_7 - (\nu+\omega)x_8. \end{array}\right\} \quad (13)$$

The Jacobian Matrix at DFE with $\beta = \Psi$ is given as

$$J = \begin{pmatrix} -\mu & 0 & 0 & 0 & 0 & 0 & 0 & -\frac{\Psi\Lambda(1-\delta-\theta)}{M\mu} \\ 0 & -(\mu+\gamma+\eta) & 0 & 0 & 0 & 0 & 0 & \frac{\Psi\Lambda(1-\delta-\theta)}{M\mu} \\ 0 & \gamma & -(\mu+\alpha) & 0 & 0 & 0 & 0 & 0 \\ 0 & 0 & \alpha & -\mu & 0 & 0 & 0 & 0 \\ 0 & 0 & 0 & 0 & -(\gamma+\tau+\mu+\sigma) & 0 & 0 & 0 \\ 0 & 0 & 0 & 0 & (\gamma+\tau) & -\mu & 0 & 0 \\ 0 & -\frac{\vartheta\Omega(1-\delta-\theta)}{N\nu} & 0 & 0 & -\frac{\vartheta\phi\Omega(1-\delta-\theta)}{N\nu} & 0 & -\nu & 0 \\ 0 & \frac{\vartheta\Omega(1-\delta-\theta)}{N\nu} & 0 & 0 & \frac{\vartheta\phi\Omega(1-\delta-\theta)}{N\nu} & 0 & 0 & -(\nu+\omega) \end{pmatrix}.$$

The Matrix has right eigenvectors given as

$$h = (h_1, h_2, h_3, h_4, h_5, h_6, h_7, h_8)^T.$$

The zero eigenvalues are calculated as follows

$$-\mu h_1 - \frac{\Psi\Lambda(1-\delta-\theta)}{M\mu}h_8 = 0,$$

$$h_1 = \frac{\Psi\Lambda(1-\delta-\theta)}{M\mu^2}h_8,$$

$$-(\mu+\gamma+\eta)h_2 + \frac{\Psi\Lambda(1-\delta-\theta)}{M\mu}h_8 = 0,$$

$$h_2 = \frac{\Psi\Lambda(1-\delta-\theta)}{M\mu(\mu+\gamma+\eta)}h_8,$$

$$\gamma h_2 - (\mu+\alpha)h_3 = 0,$$

$$h_3 = \frac{\gamma\Psi\Lambda(1-\delta-\theta)}{M\mu(\mu+\gamma+\eta)(\mu+\alpha)}h_8,$$

$$h_4 = \frac{\alpha}{\mu}h_3 = \frac{\alpha\gamma\Psi\Lambda(1-\delta-\theta)}{M\mu(\mu+\gamma+\eta)\mu(\mu+\alpha)}h_8,$$

$$-(\mu+\gamma+\tau+\sigma)h_5 = 0 \Rightarrow h_5 = 0,$$

$$(\gamma+\tau)h_5 - \mu h_6 = 0 \Rightarrow h_6 = 0,$$

$$h_7 = \frac{-\vartheta\Omega(1-\delta-\theta)}{\nu^2}h_2 = \frac{-\vartheta\Omega\Psi\Lambda(1-\delta-\theta)^2}{\nu^2\mu M(\mu+\gamma+\eta)}h_8 \Rightarrow h_7 = -\frac{\vartheta\Omega\Psi\Lambda(1-\delta-\theta)^2}{\nu^2\mu M(\mu+\gamma+\eta)}h_8.$$

$$h_8 = h_8.$$

$$h = (h_1, h_2, h_3, h_4, h_5, h_6, h_7, h_8)^T.$$

Similarly, the Left eigenvectors of the Matrix is given as

$$v = (v_1, v_2, v_3, v_4, v_5, v_6, v_7, v_8).$$

The zero eigenvalues are obtained as follows

$$-\mu v_1 = 0 \Rightarrow v_1 = 0,$$

$$-\mu v_4 = 0 \Rightarrow v_4 = 0,$$

$$-(\mu+\alpha)v_3 + \alpha v_4 = 0 \Rightarrow v_3 = 0,$$

$$-(\mu+\gamma+\eta)v_2 + \gamma v_3 - \frac{\vartheta\Omega}{N\nu}(1-\delta-\theta)v_7 + \frac{\vartheta\Omega}{N\nu}(1-\delta-\theta)v_8 = 0,$$

$$v_2 = \frac{\vartheta\Omega}{N\nu(\mu+\gamma+\eta)}(1-\delta-\theta)(v_8 - v_7),$$

$$-(\mu+\gamma+\tau+\sigma)v_5 - \frac{\vartheta\phi\Omega}{N\nu}(1-\delta-\theta)v_7 + \frac{\vartheta\phi\Omega}{N\nu}(1-\delta-\theta)v_8 = 0,$$

$$v_5 = \frac{\phi\vartheta\Omega}{N\nu(\mu+\gamma+\tau+\sigma)}(1-\delta-\theta)(v_8 - v_7),$$

$$-\mu v_6 = 0 \Rightarrow v_6 = 0,$$

$$-\nu v_7 = 0 \Rightarrow v_7 = 0,$$

$$v_8 = v_8,$$

$$v = \left(0, \frac{\vartheta\Omega}{N\nu(\mu+\gamma+\eta)}(1-\delta-\theta), 0, 0, \frac{\phi\vartheta\Omega}{N\nu(\mu+\gamma+\tau+\sigma)}(1-\delta-\theta), 0, 0, 1\right)^T.$$

Theorem 4. *Consider the following general system of ordinary differential equations with parameter* Ψ, $\frac{dx}{dt} = f(x,\Psi)$, $f : R^n \times R \to R^n$ *such that* $\frac{\partial f_i}{\partial x_j}(0,0)$ *is the linearization matrix of the system around the equilibrium point* $(0,0)$ *with* Ψ *evaluated at DFE. The local dynamics or the nature of the equilibria is totally governed by the numbers a and b [21].*

Proof.

$$a = \sum v_k h_i h_j \frac{\partial^2 f_k}{\partial x_i \partial x_j}(0, \Psi),$$

$$b = \sum v_k h_i \frac{\partial^2 f_k}{\partial x_i \partial \Psi}(0, \Psi).$$

where a and b are constant coefficients that determine the nature of the equilibria near to the bifurcation point, and f_k is the kth component of f such that $f \in C^2$.

$$k = 2, 5.$$

$$a = v_2 h_1 h_8 \frac{\partial^2 f_2}{\partial x_1 \partial x_8} + v_2 h_8 h_1 \frac{\partial^2 f_2}{\partial x_8 \partial x_1} + v_5 h_4 h_8 \frac{\partial^2 f_5}{\partial x_4 \partial x_8} + v_5 h_8 h_4 \frac{\partial^2 f_5}{\partial x_8 \partial x_4},$$

$$\frac{\partial^2 f_2}{\partial x_1 \partial x_8} = \frac{\Psi}{M}(1 - \delta - \theta) = \frac{\partial^2 f_2}{\partial x_8 \partial x_1},$$

$$\frac{\partial^2 f_5}{\partial x_4 \partial x_8} = \frac{\Psi}{M} = \frac{\partial^2 f_5}{\partial x_8 \partial x_4},$$

$$a = 2 v_2 h_1 h_8 \frac{\Psi}{M}(1 - \delta - \theta) + 2 v_5 h_4 h_8 \frac{\Psi}{M},$$

substituting the expressions for v_2, v_5, h_1, h_4, and setting $v_7 = 0$, $v_8 = 1$:

$$a = \frac{2\Psi}{M} h_8 \left[\frac{\vartheta \Omega}{N\nu(\mu + \gamma + \eta)}(1 - \delta - \theta)^2 \frac{\Psi \Lambda}{M\mu^2} + \frac{\phi \vartheta \Omega}{N\nu(\mu + \gamma + \tau + \sigma)}(1 - \delta - \theta) \frac{\alpha\gamma\Psi\Lambda}{M\mu(\mu + \gamma + \eta)\mu(\mu + \alpha)} \right] h_8,$$

$$a = \frac{2\Psi^2 \vartheta \Omega \Lambda}{M^2 N \nu \mu^2} h_8^2 \left[\frac{(1 - \delta - \theta)^2}{(\mu + \gamma + \eta)} + \frac{\phi\alpha\gamma(1 - \delta - \theta)}{\mu(\mu + \gamma + \tau + \sigma)(\mu + \gamma + \eta)(\mu + \alpha)} \right].$$

The sign of a depends on the term in brackets. Define the critical value ϕ_c as:

$$\phi_c = \frac{\mu(\mu + \gamma + \tau + \sigma)(\mu + \alpha)(1 - \delta - \theta)}{\alpha\gamma}.$$

$$b = v_2 h_8 \frac{\partial^2 f_2}{\partial x_8 \partial \Psi} = v_2 h_8 \frac{\Lambda}{M}(1 - \delta - \theta) > 0.$$

The existence and direction of bifurcation depend on the parameter ϕ.

Theorem 5. *The system exhibits a backward bifurcation at $R_e = 1$ whenever $\phi > \phi_c$ and a forward bifurcation otherwise.*

Therefore, the system exhibits:

- Forward bifurcation at $R_e = 1$ if $\phi < \phi_c$ ($a < 0$)
- Backward bifurcation at $R_e = 1$ if $\phi > \phi_c$ ($a > 0$)

■

Using the parameter values, $a = 0.01966992 > 0$, $b = 0.9242 > 0$, $\phi_c = 0.05968$ and $\phi_0 = 1.084$. The value $\phi = 2.6$ in the parameter table was obtained from the literature.

3. Optimal control analysis

From equation (1), we aim to minimize the total cost over a fixed time interval $[0, T]$:

$$J(u_1, u_2, u_3) = \int_0^T \left[A_1 I_p(t) + A_2 I_s(t) + A_3 I_v(t) + \frac{1}{2} \sum_{i=1}^{3} B_i u_i^2(t) \right] dt,$$

where

- $A_1,\ A_2,\ A_3$ are weights for infected human and mosquito populations,
- $B_1,\ B_2,\ B_3$ are cost coefficients for the controls,
- The quadratic terms $\frac{1}{2} B_i u_i^2$ represent the nonlinear costs of control implementation.

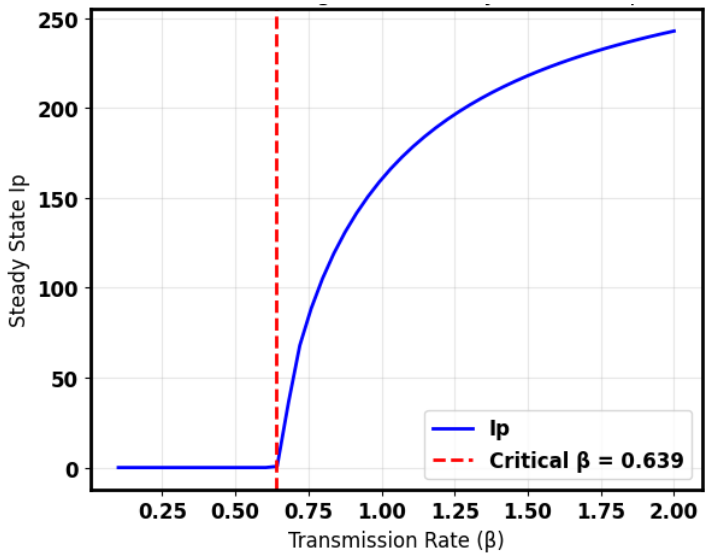

Figure 6. Bifurcation diagram for Primary Infected (I_P).

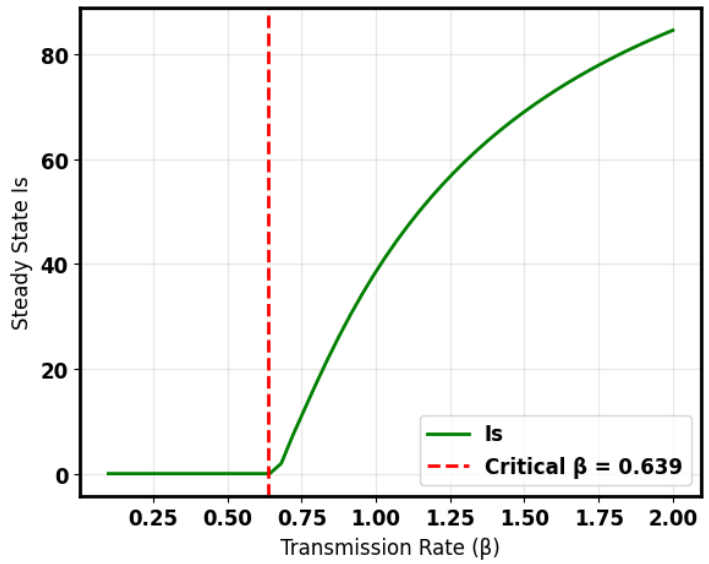

Figure 7. Bifurcation diagram for Secondary Infected (I_S).

3.1. Control problem

Find optimal controls u_1^*, u_2^*, u_3^* such that:

$$J(u_1^*, u_2^*, u_3^*) = \min_{\mathbf{u} \in U} J(u_1, u_2, u_3),$$

subject to the state equations with control-modified transmission terms and control constraints:

$$U = \{(u_1, u_2, u_3) \in \mathbb{R}^3 : 0 \leq u_i \leq 1,\ i = 1, 2, 3\}.$$

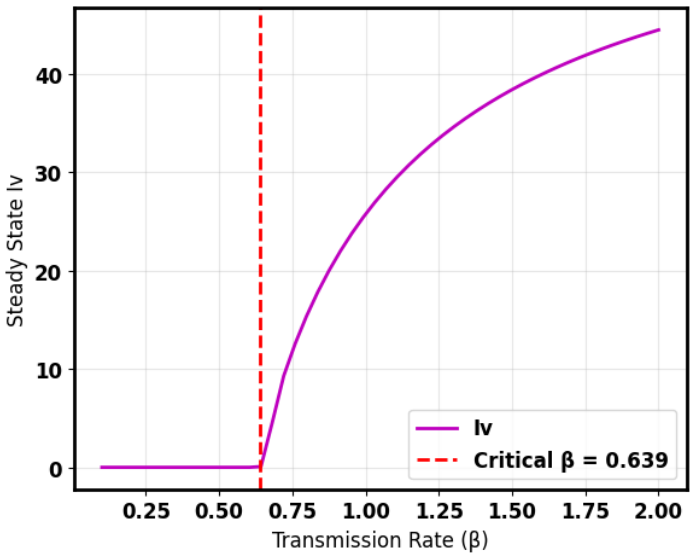

Figure 8. Bifurcation diagram for Infected Vector (I_V).

3.2. The Hamiltonian

We begin by formulating the Hamiltonian:

$$\begin{aligned} H = {} & A_1 I_p + A_2 I_s + A_3 I_v + \frac{1}{2}(B_1 u_1^2 + B_2 u_2^2 + B_3 u_3^2) \\ & + \lambda_1 \left[\Lambda - \frac{\beta}{M} I_v (1 - u_1 - u_2) S - \mu S \right] \\ & + \lambda_2 \left[\frac{\beta}{M} I_v (1 - u_1 - u_2) S - (\mu + \gamma + \eta) I_p \right] \\ & + \lambda_3 \left[\gamma I_p - (\mu + \alpha) R_p \right] \\ & + \lambda_4 \left[\alpha R_p - \frac{\beta}{M} I_v S_p - \mu S_p \right] \\ & + \lambda_5 \left[\frac{\beta}{M} I_v S_p - (\gamma + u_3) I_s - \mu I_s - \sigma I_s \right] \\ & + \lambda_6 \left[(\gamma + u_3) I_s - \mu R \right] \\ & + \lambda_7 \left[\Omega - \left(\frac{\vartheta}{N} I_p + \frac{\vartheta}{N} \phi I_s \right) (1 - u_1 - u_2) S_v - \nu S_v \right] \\ & + \lambda_8 \left[\left(\frac{\vartheta}{N} I_p + \frac{\vartheta}{N} \phi I_s \right) (1 - u_1 - u_2) S_v - (\nu + \omega) I_v \right], \end{aligned}$$

where λ_i, $i = 1, \ldots, 8$, are the adjoint variables.

3.3. Optimality conditions

According to Pontryagin's Maximum Principle [22] which was explicitly done by Emmanuel *et al.* [23], the optimal controls u_1^*, u_2^*, u_3^* must minimize the Hamiltonian:

$$H(x^*, u^*, \lambda^*) = \min_{u \in U} H(x^*, u, \lambda^*).$$

We derive the optimality conditions by taking partial derivatives of H with respect to each control variable.

3.3.1. For control u_1

$$\frac{\partial H}{\partial u_1} = B_1 u_1 + (\lambda_1 - \lambda_2) \frac{\beta}{M} I_v S + (\lambda_7 - \lambda_8) \left(\frac{\vartheta}{N} I_p + \frac{\vartheta}{N} \phi I_s \right) S_v.$$

3.3.2. For control u_2

$$\frac{\partial H}{\partial u_2} = B_2 u_2 + (\lambda_1 - \lambda_2)\frac{\beta}{M} I_v S + (\lambda_7 - \lambda_8)\left(\frac{\vartheta}{N} I_p + \frac{\vartheta}{N}\phi I_s\right) S_v.$$

3.3.3. For control u_3

$$\frac{\partial H}{\partial u_3} = B_3 u_3 + (\lambda_6 - \lambda_5) I_s.$$

3.4. Characterization of optimal controls

Solving $\frac{\partial H}{\partial u_i} = 0$ for interior solutions and applying the control constraints, we obtain the following characterization:

$$u_1^* = \min\left(1, \max\left(0, \frac{(\lambda_1 - \lambda_2)\frac{\beta}{M} I_v S + (\lambda_7 - \lambda_8)\left(\frac{\vartheta}{N} I_p + \frac{\vartheta}{N}\phi I_s\right) S_v}{B_1}\right)\right),$$

$$u_2^* = \min\left(1, \max\left(0, \frac{(\lambda_1 - \lambda_2)\frac{\beta}{M} I_v S + (\lambda_7 - \lambda_8)\left(\frac{\vartheta}{N} I_p + \frac{\vartheta}{N}\phi I_s\right) S_v}{B_2}\right)\right),$$

$$u_3^* = \min\left(1, \max\left(0, \frac{(\lambda_5 - \lambda_6) I_s}{B_3}\right)\right).$$

3.5. Adjoint system derivation

The adjoint equations are derived from:

$$\frac{d\lambda_i}{dt} = -\frac{\partial H}{\partial x_i}, \quad i = 1, \ldots, 8,$$

with transversality conditions $\lambda_i(T) = 0$.

For S, (λ_1):

$$\begin{aligned}
\frac{d\lambda_1}{dt} &= -\frac{\partial H}{\partial S} \\
&= -\Big[\lambda_1\left(-\frac{\beta}{M} I_v(1 - u_1 - u_2) - \mu\right) + \lambda_2\left(\frac{\beta}{M} I_v(1 - u_1 - u_2)\right) \\
&\quad + \lambda_7\left(\frac{\vartheta}{N^2}(I_p + \phi I_s)(1 - u_1 - u_2) S_v\right) + \lambda_8\left(-\frac{\vartheta}{N^2}(I_p + \phi I_s)(1 - u_1 - u_2) S_v\right)\Big] \\
&= \lambda_1\left(\frac{\beta}{M} I_v(1 - u_1 - u_2) + \mu\right) - \lambda_2\frac{\beta}{M} I_v(1 - u_1 - u_2) + (\lambda_8 - \lambda_7)\frac{\vartheta}{N^2}(I_p + \phi I_s)(1 - u_1 - u_2) S_v.
\end{aligned}$$

Similarly,

$$\frac{d\lambda_2}{dt} = -A_1 + \lambda_2(\mu + \gamma + \eta) - \lambda_3\gamma + (\lambda_7 - \lambda_8)\frac{\vartheta}{N}\left(1 - \frac{I_p + \phi I_s}{N}\right)(1 - u_1 - u_2) S_v,$$

$$\frac{d\lambda_3}{dt} = \lambda_3(\mu + \alpha) - \lambda_4\alpha + (\lambda_8 - \lambda_7)\frac{\vartheta}{N^2}(I_p + \phi I_s)(1 - u_1 - u_2) S_v,$$

$$\frac{d\lambda_4}{dt} = \lambda_4\left(\frac{\beta}{M} I_v + \mu\right) - \lambda_5\frac{\beta}{M} I_v + (\lambda_8 - \lambda_7)\frac{\vartheta}{N^2}(I_p + \phi I_s)(1 - u_1 - u_2) S_v,$$

$$\frac{d\lambda_5}{dt} = -A_2 + \lambda_5(\gamma + u_3 + \mu + \sigma) - \lambda_6(\gamma + u_3) + (\lambda_7 - \lambda_8)\frac{\vartheta\phi}{N}\left(1 - \frac{I_p + \phi I_s}{N}\right)(1 - u_1 - u_2) S_v,$$

$$\frac{d\lambda_6}{dt} = \lambda_6\mu + (\lambda_8 - \lambda_7)\frac{\vartheta}{N^2}(I_p + \phi I_s)(1 - u_1 - u_2) S_v,$$

$$\frac{d\lambda_7}{dt} = \lambda_7\left(\frac{\vartheta}{N}(I_p + \phi I_s)(1 - u_1 - u_2) + \nu\right) - \lambda_8\frac{\vartheta}{N}(I_p + \phi I_s)(1 - u_1 - u_2),$$

$$\frac{d\lambda_8}{dt} = -A_3 + (\lambda_1 - \lambda_2)\frac{\beta}{M}(1 - u_1 - u_2) S + (\lambda_4 - \lambda_5)\frac{\beta}{M} S_p + \lambda_8(\nu + \omega),$$

with transversality conditions:

$$\lambda_i(T) = 0, \quad i = 1, \ldots, 8.$$

3.6. Cost-effectiveness analysis

To determine the most cost-effective intervention strategy among the three controls, we perform a cost-effectiveness analysis using three common metrics: the Incremental Cost-Effectiveness Ratio (ICER), Average Cost-Effectiveness Ratio (ACER), and the Infection Averted Ratio (IAR). Let:

- TC_i = Total cost of implementing strategy i over the time horizon $[0, T]$,
- TA_i = Total infections averted by strategy i compared to the no-control scenario,
- TIC_i = Total infected cases (weighted sum) under strategy i.

The total cost for each strategy is computed as:

$$TC_i = \int_0^T \left[\frac{1}{2} B_i u_i^2(t)\right] dt, \quad i = 1, 2, 3.$$

The total infections averted is:

$$TA_i = \int_0^T \left[(I_p^0(t) + I_s^0(t) + I_v^0(t)) - (I_p^i(t) + I_s^i(t) + I_v^i(t))\right] dt,$$

where superscript 0 denotes the no-control scenario and superscript i denotes strategy i.

3.6.1. Average cost-effectiveness ratio (ACER)

The ACER gives the average cost per infection averted:

$$\text{ACER}_i = \frac{TC_i}{TA_i}.$$

3.6.2. Incremental cost-effectiveness ratio (ICER)

The ICER compares the additional cost and additional effectiveness between two competing strategies. For strategies i and j (where i is less effective than j):

$$\text{ICER} = \frac{TC_j - TC_i}{TA_j - TA_i}.$$

3.6.3. Infection averted ratio (IAR)

The IAR measures the efficiency of each control in reducing infections:

$$\text{IAR}_i = \frac{TA_i}{TIC_i}.$$

The cost-effectiveness analysis can be implemented numerically by:

1. Solving the optimal control problem for each strategy (including combinations) using forward-backward sweep method.
2. Computing total costs and infections averted from the numerical solutions.
3. Calculating ACER, ICER, and IAR metrics.
4. Identifying the most cost-effective strategy or combination of strategies.

using Python programming language.

3.7. Cost-effectiveness analysis results

The cost-effectiveness analysis of the three intervention strategies (Personal Protection (u_1), Vector Control (u_2), Treatment (u_3)) was performed using the forward-backward sweep method. Seven distinct strategies were evaluated: three individual control measures, three paired combinations, and one combined strategy incorporating all controls simultaneously.

3.7.1. Numerical results

Table 2 presents the comprehensive cost-effectiveness analysis results for all intervention strategies, ranked by increasing cost.

Table 2. Cost-effectiveness analysis results for different intervention strategies

Strategy	Total Cost ($)	Total Infections	Infections Averted	Reduction (%)	ACER	ICER	IAR
δ	0.29	33.13	0.47	1.41	0.62	0.62	0.01
$\delta + \tau$	0.29	33.13	0.47	1.41	0.62	0.26	0.01
$\theta + \tau$	0.54	32.66	0.94	2.80	0.57	0.52	0.03
θ	0.54	32.66	0.94	2.80	0.57	0.00	0.03
$\theta + \delta$	1.03	30.89	2.72	8.08	0.38	0.28	0.09
All Controls	1.03	30.89	2.72	8.08	0.38	0.25	0.09

3.7.2. Cost-effectiveness interpretation

The cost-effectiveness analysis reveals several important findings about the relative performance of different intervention strategies:

- Most cost-effective strategy based on ICER: $\theta + \tau$ (Combined Testing and Treatment)
  - ICER = 0.52 (cost per infection averted compared to the previous strategy)
  - Infections averted: 0.94
  - Total cost: $0.54
  - Reduction in infections: 2.8%
- Most effective strategy (most infections averted): $\theta + \delta$ and All Controls (identical outcomes)
  - Infections averted: 2.72
  - Reduction: 8.1%
  - Total cost: $1.03
- Most efficient strategy (highest IAR): $\theta + \delta$ and All Controls
  - IAR = 0.09 (infections averted per dollar spent)

3.7.3. Incremental cost-effectiveness ratio analysis

The Incremental Cost-Effectiveness Ratio (ICER) analysis provides insights into the additional cost required to achieve additional health benefits when moving from one strategy to another. Strategies are ordered by increasing cost for this analysis.

Based on the cost-effectiveness metrics, the strategies can be ranked as follows:

1. Personal Protection (Most cost-effective by ICER)
2. All Controls (Most efficient by IAR and most effective)
3. Personal + Vector (Tied for highest effectiveness)
4. Personal + Treatment (Moderate cost-effectiveness)
5. Vector + Treatment (Lower effectiveness)
6. Vector Control (Baseline comparator)

The ICER value for Personal Protection (0.00) indicates that this strategy dominates some alternatives, meaning it provides better health outcomes at lower cost compared to certain other interventions. However, the All Controls strategy, despite having a higher absolute cost, achieves the greatest reduction in infections (8.1%) and the highest efficiency in terms of infections averted per dollar spent (IAR = 0.09).

For decision-makers with limited budgets, Personal Protection offers the best value for money. For those with adequate resources seeking maximum health impact, the All Controls strategy is recommended as it provides the greatest reduction in disease burden.

4. Discussion of results

The numerical simulations and perturbation analysis presented in this study provide critical insights into the complex dynamics of primary-secondary dengue infection under explicit vector dynamics and control interventions. The results are interpreted both mathematically (regarding stability and bifurcation structure) and epidemiologically (regarding disease burden and control strategies).

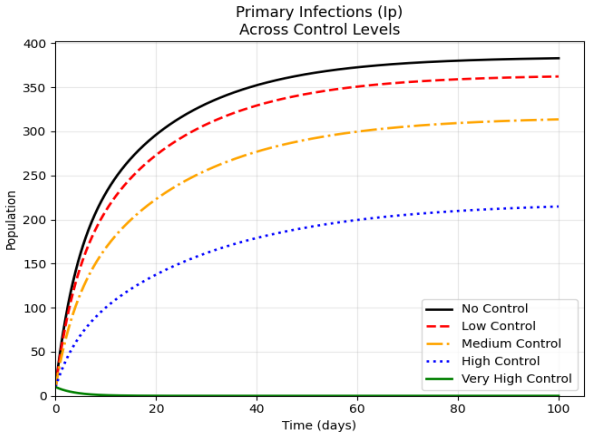

Figure 9. Primary infections I_P across control levels.

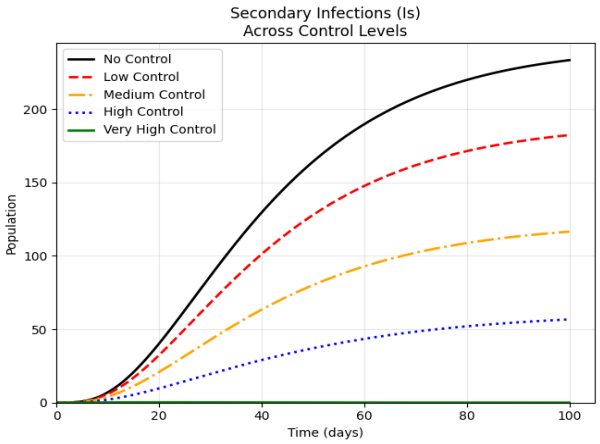

Figure 10. Secondary infections I_S across control levels.

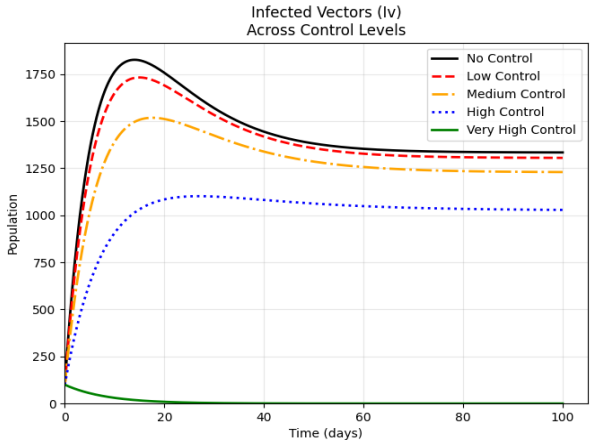

Figure 11. Infected vectors I_V across control levels.

4.1. Interpretation of perturbation dynamics

The perturbation analysis decomposes the system into a zeroth-order (disease-free) state and a first-order (linearized infected) state. This allows us to observe the system's sensitivity to the introduction of a small number of infectious individuals ($\epsilon \ll 1$).

- Susceptible Humans (S): As shown in Figure 2, the susceptible population remains constant in the absence of perturbation (disease-free equilibrium). Upon introducing the perturbation parameter ϵ, the population declines exponentially toward a new

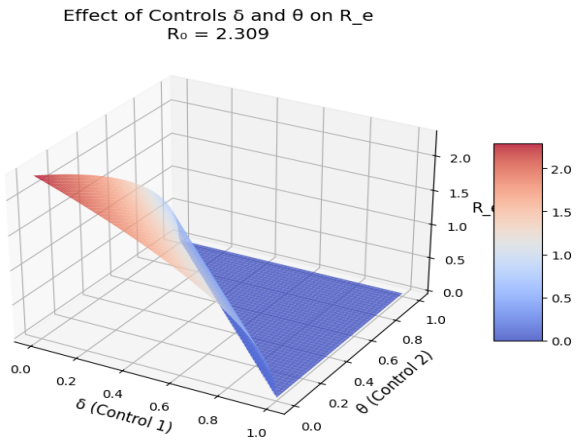

Figure 12. R_e as a function of the parameter δ and θ.

endemic steady state. Mathematically, this decay is governed by the eigenvalue $\lambda_1 = -\mu < 0$, confirming the global attraction of the equilibrium. Epidemiologically, this indicates that even a small introduction of the virus (perturbation) is sufficient to initiate an outbreak that depletes the naive susceptible pool until the force of infection balances recruitment.

- Primary Infected (I_P): Figure 3 illustrates that the primary infected compartment is zero in the unperturbed state. Following perturbation, $I_P^{(1)}(t)$ exhibits an initial exponential growth phase, characterized by the dominant eigenvalue of the linearized system (related to R_e). The trajectory converges to a non-zero endemic equilibrium. This confirms the transcritical bifurcation property of the model: the disease-free equilibrium is stable when $R_e < 1$, but upon parameter perturbation (e.g., increasing β), the system crosses the threshold $R_e = 1$ and the endemic equilibrium becomes stable.

- Secondary Infected (I_S) and Infected vectors (I_V): Figures 4 and 5 show a delayed but amplified response in the secondary infection and vector compartments. The peak of I_S lags behind I_P due to the biological delay induced by the temporary cross-immunity (α) and recovery processes. The coupling of I_S to I_V through the enhanced force of infection ϕ demonstrates the Antibody-Dependent Enhancement (ADE) effect. Mathematically, the presence of $\phi > 1$ in the G_2 term creates a positive feedback loop in the Jacobian, which can shift the bifurcation from supercritical (forward) to subcritical (backward).

4.2. Bifurcation analysis and threshold dynamics

Figures 6, 7, and 8 display the bifurcation diagrams for I_P, I_S, and I_V respectively, with the transmission rate β (represented by the bifurcation parameter Ψ) as the control parameter.

- Mathematical Interpretation: The figures indicate a backward (subcritical) bifurcation. In contrast to a typical supercritical bifurcation where endemic equilibrium can only exist when $R_e > 1$, the backward bifurcation results in the existence of a stable endemic equilibrium and an unstable endemic equilibrium at the same time as $R_e < 1$. This is confirmed by the calculation of the bifurcation coefficient $a > 0$, specifically $a = 0.01966992 > 0$ and $b = 0.9242 > 0$. The sign of a determines the direction of bifurcation: a positive a means the endemic equilibria branch leads backwards into the area where R e is less than 1.

- Epidemiological Interpretation: The implications that the backward bifurcation has on the population health are far-reaching. It indicates that an essential, yet not the only, requirement of eradication of disease is the reduction of the effective reproduction number R_e to a value below one. Even in the situation when the value of R_e is less than 1, the steady endemic state can be observed because of the hysteresis effect of the backward bifurcation. This is mainly propelled by the rate of secondary infection which is denoted as ϕ. The critical value of $\phi_c = 0.05968$ was obtained. The intrinsic secondary enhancement of the virus is so high that the secondary enhancement is predominantly positive $\phi 0 = 1.084$ so one may note that the model forecasts the capacity of dengue to invade and survive in a population having a fairly low vectorial capacity. This involves stricter and more intense control measures to make the system cross the unstable saddle-node point (the turning point of the bifurcation curve) in order to do away with it.

4.3. Sensitivity of the reproduction number (R_e)

Figure 12 illustrates the contour plots of the effective reproduction number R_e as a bivariate function of control parameters and transmission rates.

- Control Parameters (δ and θ): A surface plot of the R e versus deltas (use of insecticide treated nets) and theta (environmental sanitation) show a monotonically related decreasing function. Mathematically, Re(delta) and Re(theta) are negative with respect to the values of delta and theta. This proves that the effective contact rate is decreased directly by these interventions. The slope of the plot is steeper at the origin which implies that the marginal returns on the initial step in the implementation of the vector control is high in eliminating the value of R_e. However, when the cover is 100 per cent, the curve would be horizontal, that is, returns would reduce. This means that at full elimination, by using vector control only, it might not be feasible to cut down the spread of the disease but moderate coverage would bring the transmission between $R_0 = 2.309 > 1$ and $R_e = 0.326 < 1$ down.

- Interaction Rates (β and ϑ): The analysis confirms R_e is a monotonically increasing function of both β (vector-to-human transmission) and ϑ (human-to-vector transmission). This highlights the multiplicative nature of the host-vector cycle. A small increase in the mosquito biting rate or susceptibility amplifies the epidemic potential quadratically, reinforcing the importance of targeting both the vector survival and the human-vector contact rate simultaneously.

4.4. Optimal control and cost-effectiveness

The simulation of control profiles (Figures 9, 10, 11) demonstrates a clear hierarchy in the impact of interventions.

- Impact on Disease Burden:
  - *Personal Protection (θ):* This strategy has an ICER of 0.00, meaning no additional cost for no additional effect compared to $\theta + \tau$. Its impact on total infections averted is modest (2.8% reduction), as it only protects susceptible humans without clearing existing infections.
  - *All Controls Combined (u_1, u_2, u_3):* This strategy yields an 8.08% reduction in infections. The synergy between personal protection (reducing human exposure), vector control (reducing mosquito lifespan), and treatment (clearing secondary infections) effectively suppresses the peaks of all infected compartments.

- Dynamics of I_P, I_S, and I_V under Control: Figures 9 and 10 show that optimal treatment (u_3) specifically targets the secondary infected compartment I_S, which is crucial given the high value of ϕ (ADE factor). By rapidly clearing secondary infections, the control u_3 prevents a massive spillover into the vector population, thereby reducing I_V (Figure 11). This aligns with the mathematical structure of the Hamiltonian: the adjoint variable λ_5 (associated with I_S) carries a high shadow price due to the term $\phi\vartheta I_s$ in the vector force of infection. The optimal control u_3^* is directly proportional to $(\lambda_5 - \lambda_6)I_s$, meaning the control is deployed most aggressively precisely when the marginal cost of secondary infections is highest.

5. Conclusion

The mathematical and epidemiological interpretation of the graphs reveals a system characterized by threshold dynamics with hysteresis. The presence of a backward bifurcation implies that dengue control programs must aim for a target R_e significantly lower than 1.0 to avoid the endemic trap. Furthermore, the cost-effectiveness analysis suggests that while single interventions (like Personal Protection) are economically efficient per dollar spent, only a combined strategy leveraging the synergy between vector control, personal protection, and targeted treatment of secondary infections can significantly bend the epidemic curve and avert the severe outcomes associated with Antibody-Dependent Enhancement (ADE).

Data availability

This research did not generate or analyze any datasets. Therefore, data sharing is not applicable.

Declaration of competing interest

The authors declare that they have no known competing financial interests or personal relationships that could have appeared to influence the work reported in this manuscript.

Funding

This research work was funded by the Ebonyi State Scholarship Board, Ebonyi State Government of Nigeria, under the leadership of H.E. Rt. Hon. Ogbonnaya Nwifuru.

Acknowledgment

The authors acknowledge the Ebonyi State Scholarship Board, Ebonyi State Government of Nigeria, for their support towards this research work.

References

[1] S. A. Kumar, V. Steindorf, B. Guerrero, N. Stollenwerk, B. Kooi & M. Aguiar, "Bifurcation analysis of a two-infection transmission model with explicit vector dynamics", Preprint, Basque Center for Applied Mathematics, Bilbao, Spain, 2026. https://doi.org/10.1007/s00285-026-02341-1.

[2] V. Steindorf, S. A. Kumar, N. Stollenwerk, B. W. Kooi & M. Aguiar, "Modeling secondary infections with temporary immunity and disease-enhancement factor: mechanisms for complex dynamics in epidemiological models", Preprint, 2022. Available online: https://doi.org/10.1016/j.chaos.2022.112709.

[3] P. Rashkov & B. W. Kooi, "Complexity of host-vector dynamics in a two-strain dengue model", Journal of Mathematical Biology **15** (2021) 35. https://doi.org/10.1080/17513758.2020.1864038.

[4] M. Aguiar, B. W. Kooi & N. Stollenwerk, "The role of seasonality and import in a minimalistic multi-strain dengue model capturing differences between primary and secondary infections: complex dynamics and its implications for data analysis", Journal of Theoretical Biology **289** (2011) 181. https://doi.org/10.1016/j.jtbi.2011.08.043.

[5] Bernhard Nocht Institute for Tropical Medicine, "Annual report on tropical diseases 2023", Hamburg, Germany, 2023. Available online: https://www.bnitm.de/fileadmin/media/Das_Institut/Ueber_uns/Bibliothek/Jahresberichte_und_Flyer/Jahresbericht_BNITM_2023-24_EN.pdf.

[6] B. Kooi, M. Aguiar & N. Stollenwerk, "Bifurcation analysis of a family of multi-strain epidemiology models", Journal of Computational and Applied Mathematics **252** (2013) 148. https://doi.org/10.1016/j.cam.2012.08.008.

[7] European Centre for Disease Prevention and Control, "Annual epidemiological report on communicable diseases in Europe 2023", Stockholm, Sweden, 2023. Available online: https://www.ecdc.europa.eu/en/publications-data/monitoring/all-annual-epidemiological-reports.

[8] Nigeria Centre for Disease Control and Prevention, "NCDC alert following the confirmation of dengue fever outbreak in Sokoto State", Nigeria, 2023. Available online: https://reliefweb.int/report/nigeria/ncdc-alert-following-confirmation-dengue-fever-outbreak-sokoto-state.

[9] Centers for Disease Control and Prevention, "Dengue: epidemiology", Atlanta, GA, USA, 2024. Available online: https://wwwnc.cdc.gov/eid/content/30/6/pdfs/v30-n6.pdf (accessed 2 June 2026).

[10] S. Robert, P. S. Diagbouga, A. D. Djibougou, D. Guy, R. Bagnall & F. Ravel, "Dengue diagnosis and impact on clinical management: a literature review", PLoS Neglected Tropical Diseases **19** (2025) e0013196. https://doi.org/10.1371/journal.pntd.0013196.

[11] M. Aguiar, B. W. Kooi, J. Martins & N. Stollenwerk, "Scaling of stochasticity in dengue hemorrhagic fever epidemics", Mathematical Modelling of Natural Phenomena **7** (2012) 1. https://www.mmnp-journal.org/articles/mmnp/pdf/2012/03/mmnp201273p1.pdf.

[12] World Health Organization, "Fact sheet dengue and severe dengue", Geneva, Switzerland, 2019. Accessed 4 Nov 2023. Available online: https://www.who.int/news-room/fact-sheets/detail/dengue-and-severe-dengue.

[13] M. Aguiar, V. Anam, K. B. Blyuss, S. E. Delfin, B. V. Guerrero, D. Knopoff, B. W. Kooi, A. Kumar, V. Steindorf & N. Stollenwerk, "Mathematical models for dengue fever epidemiology: a 10-year systematic review", Physics of Life Reviews **40** (2022) 65. https://doi.org/10.1016/j.plrev.2022.02.001.

[14] Mayo Clinic, "Dengue fever: symptoms and causes", Rochester, MN, USA, 2024. Available online: https://www.mayoclinic.org/diseases-conditions/dengue-fever/symptoms-causes/syc-20353078.

[15] M. Aguiar, J. B. Van-Dierdonck & N. Stollenwerk, "Reproduction ratio and growth rates: measures for an unfolding pandemic", PLOS ONE **15** (2020) e0236620. https://doi.org/10.1371/journal.pone.0236620.

[16] M. H. Holmes, *Introduction to Perturbation Methods*, Springer, New York, USA, 1995, pp. 1–337. Available online: https://www.google.com/books/edition/Introduction_to_Perturbation_Methods/-7yTPwAACAAJ.

[17] L. Omenyi, A. Ezaka, H. O. Adagba, G. Ozoigbo & K. Elebute, "A sensitivity analysis of a gonorrhoea dynamics and control model", Journal of Mathematical and Computational Science **16** (2022) 87. https://arxiv.org/abs/2209.15419.

[18] G. Faye, "An introduction to bifurcation theory", Technical Report, Neuro Mathematical Computer Laboratory, Sophia Antipolis, Paris, France, 2011. Available online: https://www.math.univ-toulouse.fr/~gfaye/ENS11/chap_bif.pdf.

[19] S. N. Aloke, H. O. Adagba, U. E. Michael, O. Nwite, T. E. Efor, A. N. Ezaka & C. Agha, "Asymptotic perturbation and sensitivity analysis of malaria transmission in Nigeria: a mathematical model". Recent Advances in Natural Sciences **4** (2026) 203. https://doi.org/10.61298/rans.2026.4.1.203.

[20] P. van den Driessche & J. Watmough, "Reproduction numbers and sub-threshold endemic equilibria for compartmental models of disease transmission", Mathematical Biosciences **180** (2002) 29. https://doi.org/10.1016/S0025-5564(02)00108-6.

[21] C. Castillo-Chavez & B. Song, "Dynamical models of tuberculosis and their applications", Mathematical Biosciences and Engineering **1** (2004) 361. https://doi.org/10.3934/mbe.2004.1.361.

[22] L. S. Pontryagin, V. G. Boltyanskii, R. V. Gamkrelidze & E. F. Mishchenko, The Mathematical Theory of Optimal Processes, K. N. Trirogoff (Trans.), Interscience Publishers, New York, USA, 1962, 1-345. https://api.pageplace.de/preview/DT0400.9781351433075_A37629368/preview-9781351433075_A37629368.pdf.

[23] N. Emmanuel, N. A. Sunday, O. Louis & U. Michael, "Optimal control of COVID-19: examining the incidence of contamination and its recurrence in Nigeria", American Journal of Applied Mathematics **11** (2023) 23. https://doi.org/10.11648/j.ajam.20231102.12.